Template-Driven Dense Packing of Pentagonal Molecules in Monolayer Films

Daling Cui, Maryam Ebrahimi*, Jennifer M. Macleod*, and Federico Rosei*

Abstract

The integration of molecules with irregular shape into a long-range, dense and periodic lattice represents a unique challenge for the fabrication of engineered molecular scale architectures. The tiling of pentagonal molecules on a two-dimensional (2D) plane can be used as a proof-of-principle investigation to overcome this problem because basic geometry dictates that a 2D surface cannot be filled with a periodic arrangement of pentagons, a fundamental limitation that suggests that pentagonal molecules may not be suitable as building blocks for dense films. However, here we show that the 2D covalent organic framework (COF) known as COF-1 can direct the growth of pentagonal guest molecules as dense crystalline films at the solution/solid interface. We find that the pentagonal molecule corannulene adsorbs at two different sites on the COF-1 lattice, and that multiple molecules can adsorb into well-defined clusters patterned by the COF. Two types of these dense periodic packing motifs lead to a five-fold symmetry reduction compatible with translational symmetry, one of which gives an unprecedented high molecular density of 2.12 molecules/nm2.

Introduction

Molecular scale electronics is an emerging research area motivated by the increasing technical demands of the miniaturization of traditional silicon-based electronic devices.(1,2) However, efficient integration strategies for bridging hard electronics with the vast store of functional materials in the soft-molecular world are still lacking. One of the hindrances is that many functionalized single molecules have an irregular shape(3,4) which can create challenges in directing single-molecular growth, i.e., making each molecular junction addressable on two-dimensional (2D) surface. For example, the incompatibility between single molecule symmetry and translational order will produce defects and disordering. One possible method to assuage these intrinsic challenges is to use a tailored molecular template prepared by chemical synthesis to predictably position individual low-symmetry molecules, creating a pathway to realize large-scale single-molecule patterning.(5) However, few investigations can be found to date.

The dense and periodic tiling of pentagonal molecules on a 2D plane is an ideal model system to investigate the controlled placement of molecules with irregular shape into a geometry suitable for molecular devices. Five-fold symmetry is incompatible with translational symmetry. The 17 plane groups representing the tessellations of the Euclidian plane do not include five-fold symmetry(6) and the tiling of pentagons on a 2D plane must leave interstitial spaces. Dürer, Kepler, and Penrose have demonstrated a wealth of plane-filling solutions by considering regular pentagons, but all results are aperiodic or have a lower lattice symmetry.(7) These geometric considerations suggest facile formation of defects when pentagons pack densely and periodically on 2D surface by themselves.

In molecular experiments, previous observations(8−11) and simulations(12) have investigated the assembly of five-fold-symmetric shape-persistent macrocycles. The role of five-fold symmetry has also been demonstrated to be important in suppressing 3D crystallization(13) and in the formation of quasicrystals on a 2D plane.(14) However, systematic studies of close packing strategies for pentagonal molecules in the plane have exclusively addressed corannulene ($C_{20}H_{10}$, **CORA**, Scheme 1) and its derivatives.(15−20) These experimental observations also highlight the difficulty of

forming a long-range periodic densely packed crystal lattice in a flat 2D space with pentagonal molecules. Long range periodicity is solely available with lower packing density by reducing the five-fold symmetry to overcome its intrinsic mismatch with translational order;(17,18,20) otherwise, pentagons can only pack densely in locally ordered patches and different types of disorder/defects will appear over longer ranges.(16,18,19) Experimentally achieving dense packing of regular pentagonal molecules in a periodic lattice in the 2D plane is still an open question that has remained elusive using existing approaches.(12)

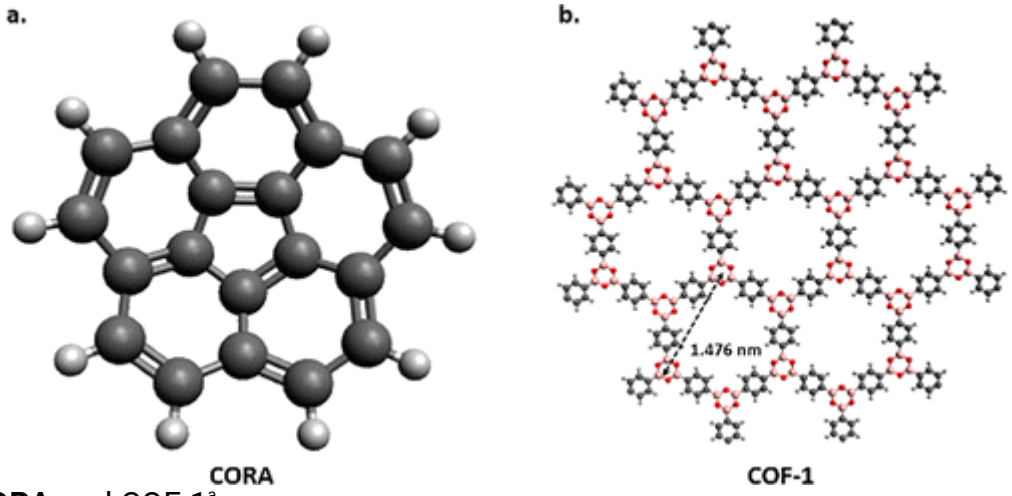

Scheme 1. **CORA** and COF-1[a]

[a](a) Top view of ball-and-stick model of **CORA** showing its C_{5v} symmetry. (b) Schematic image of single layer COF-1 (symmetry *p6mm*) which has a lattice constant of 1.476 nm when synthesized on an HOPG surface.

Here, we use a 2D host template to induce a long-range, periodic, dense self-assembly of pentagonal **CORA** guest molecules. The idea of using 2D host/guest (H/G) structures to control guest molecular deposition and layer structure has been explored for over a decade.(21−23) However, work done so far has mainly focused on high-symmetry guests like fullerene or its derivatives(24−31) and circulene molecules(32−36) in different types of 2D templates.(25,27,37,38) The symmetric compatibility in the host/guest system is also an important factor in the design of hierarchical supramolecular self-assemblies with multiple components.(38−40) In all cases, the symmetry of the guest molecules is compatible with translational symmetry.

We have used scanning tunneling microscopy (STM) to reveal the adsorption of densely packed **CORA** molecules (C_{5v} symmetry) on the host of a 2D covalent organic framework (COF-1, Scheme 1)(41) at the solution/solid interface. In these assemblies, the five-fold symmetry of **CORA** can be broken in two different ways, giving rise to a coexistence of two different long-range ordered phases. This approach can lead to an unprecedented high density periodic packing: one of the observed structures gives pentagonal molecular packing with a density of 2.12 molecules/nm^2.(18,20) The successful realization of long-range dense and periodic growth of five-fold molecules on 2D plane represents an important breakthrough for the limit set by molecular shape on the fabrication of molecular electronics.

Results and Discussion

COFs are porous crystalline materials that are characterized by robustness and customizable topology.(42) 1,4-Bezenediboronic acid monomers can form a single layer of COF-1 template through an on-surface dehydration reaction and have been used as a host to accommodate fullerene guest molecules under a range of conditions.(37,43−45) A high quality COF-1 template can be prepared on freshly cleaved highly oriented pyrolytic graphite (HOPG), producing a honeycomb mesh with a lattice parameter of 1.476 nm.(37)

After introducing the **CORA** solution, host/guest architectures were observed by STM. Two different adsorption sites can be identified. **CORA** molecules can adsorb within the pores of the COF-1 template, denoted as pore-site, as shown in Figure 1a. The rounded appearance of the pore-site **CORA** suggests a small rotational movement of the adsorbed molecules.(32) In Figure 1b, COF-1 is discernible as low-contrast hexagonal template, whereas the bright protrusions indicate that the adsorption position of **CORA** is on top of a phenyl ring of the COF-1. We denote this adsorption site as rim-site, in contrast to the top-site which corresponds to adsorption on a boroxine ring (Figure S1).(37) This observation of two different adsorption sites is similar to the C_{60}/COF-1 system(37) where the pore site provides more stable adsorption, yet guest molecules also populate a site on top of the COF lattice due to the adsorption of solvent molecules within the COF pores.(45) We suggest that the adsorbed solvent could also lead to the observed rim-site adsorption for **CORA**.

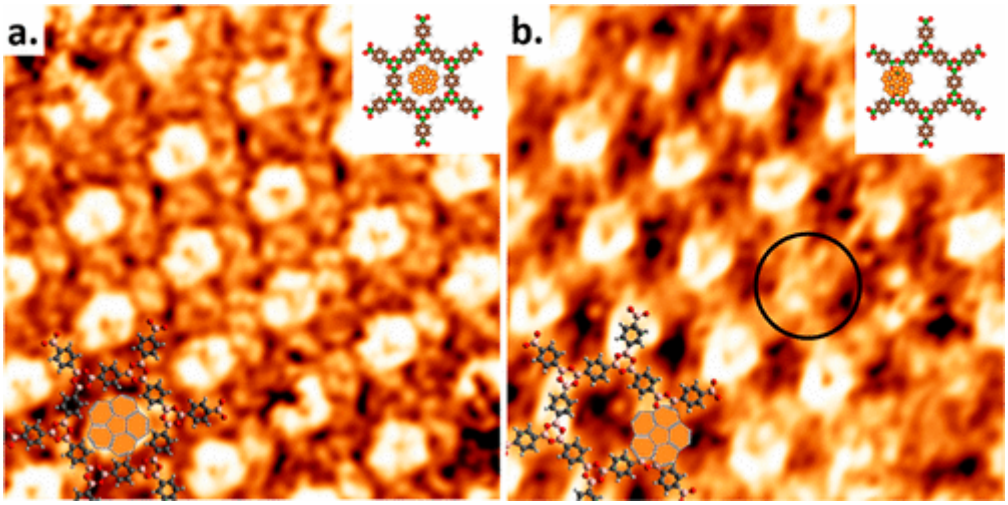

Figure 1. (a) Pore-site adsorption of **CORA** in COF-1 template. Image dimension: 6.9 × 6.9 nm^2. Tunneling conditions: V = −1800 mV, I = 50 pA. (b) Rim-site adsorption of **CORA** in COF-1. Image dimension: 7.2 × 7.2 nm^2. Tunneling conditions: V = −1800 mV, I = 50 pA. Schematics of COF-1 together with one pore-site or rim-site **CORA** are superimposed on STM images showing the adsorption position. One rim-site without adsorbed **CORA** molecule is marked by a black circle. The optimized architectures of bowl-up pore-site and bowl-down rim-site adsorption are shown in the inset images.

In both the pore-site and the rim-site, the **CORA** molecules present a dark feature in the center and bright protrusions around the edge, which is explained by a bowl-up orientation.(18,20,46,47) Our density functional theory (DFT) calculations suggest that up-oriented **CORA** is the most stable adsorption geometry in the pore-site, with an energy of −1.16 eV. (See Table 1) However, for the rim-site, down-oriented **CORA** is more stable than other geometries, corresponding to an adsorption energy of −0.84 eV. The similar appearance of both molecules can be explained by temperature-related fluctuations: at room temperature, **CORA** molecules experience a rapid (2 × 10^5 Hz) bowl to bowl inversion,(48) which is much faster than the frequency of STM scanning. The final STM appearance in the rim site is likely the result of a superposition of two orientations.(49)

Table 1. Cohesive Energy of Different Adsorption Architectures of CORA Molecule on COF-1/Graphene Bilayer

	pore-site	rim-site	top-site	trimer-II
bowl-up	–1.16 eV	–0.409 eV	–0.55 eV	–0.453 eV
bowl-down	–0.80 eV	–0.84 eV	–0.68 eV	–0.447 eV

When the density of **CORA** molecules adsorbed on the rim site of the COF-1 template increases, the submolecular features of the **CORA** become identifiable (Figure 2). This change suggests a transition from a state with some rotational freedom to an immobilized state. We assign this immobilization to the geometrical hindrance imposed by the additional adsorbed **CORA**.(50,51) Long-range STM topographies reveal the formation of coexisting periodic structures formed by two different trimer motifs (Figure S3). In both phases, the trimers pack into a honeycomb-like geometry commensurate with the COF-1 template. In the first phase (Figure 2a), three identically oriented **CORA** molecules form a D_1-symmetric trimer motif. In the second phase (Figure 2c), **CORA** molecules symmetrically orient around the center of the trimer, producing a motif with C_{3v} symmetry. These periodic arrangements of trimers define two different porous honeycomb-like lattices: a *pm*-symmetric lattice (Phase I) and a *p*3*m*1-symmetric lattice (Phase II), which are both subgroups of the *p*6*mm* symmetry of the COF-1 template. These two approaches to reduction of the five-fold symmetry are similar to a previous study of symmetry mismatching, which showed D_1 symmetric tilted **CORA** adsorption(18) and C_{3v} trimer formed by penta-*tert*-butylcorannulene on Cu(111).(17) The basic geometrical consideration suggests that **CORA** molecules in both cases are tilted and their STM appearance supports bowl-down orientation since tilted bowl-up orientation will give a mirror symmetric appearance, as shown in Figure S7.(18,19) DFT simulations (see Table 1) produce an optimized structure for Phase II, yet not for Phase I. We propose that this likely arises because of experimental conditions that we do not adequately capture in the Phase I model, such as solvent effects, which have already proven to play an important role, especially for the less-symmetric structures, in a similar system.(44) Anecdotally two different trimer motifs occur in approximately equal proportion.

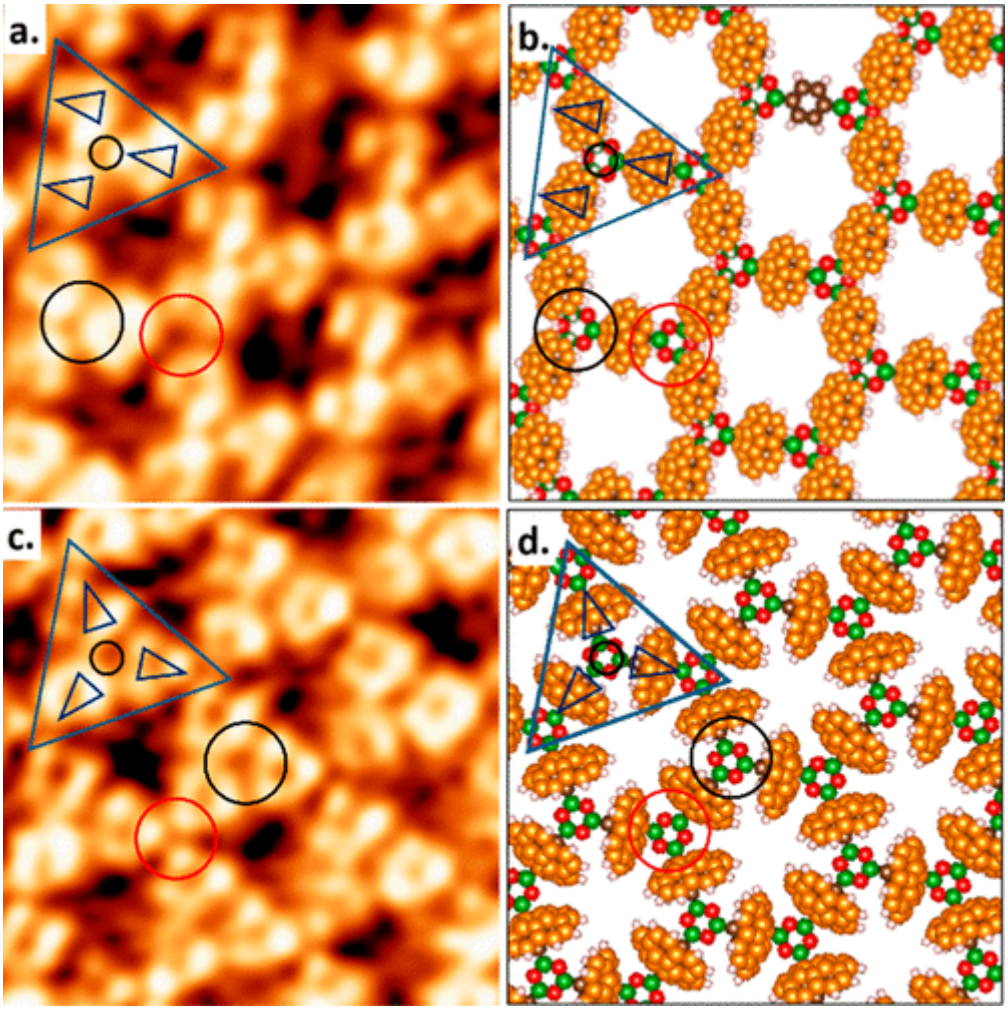

Figure 2. (a) STM image of *pm* symmetric phase I. The D_1-symmetric trimer is marked by a large open triangle and the small triangles show the parallel orientation of the **CORA** molecules. Image dimension: 4.1 × 4.1 nm^2. (b) Proposed schematic image of (a). Red and black circles are placed according to (a). (c) STM image of *p*3*m*1 symmetric phase II. The C_{3v}-symmetric trimer is marked

by a large open triangle and the small triangles show the symmetric orientation of the **CORA** molecules around the center of the trimer. Image dimension: 4.4 × 4.4 nm^2. (d) Tilted bowl-down optimized structure of (c). Red and black circles are placed according to (c). Tunneling conditions: V = −1800 mV, I = 50 pA.

In addition to these structures, other packing geometries have also been observed, including a dimer formed by two **CORA** molecules, as shown in Figure S4. There is also a possibility for coadsorption of pore-site **CORA** along with trimeric rim-site **CORA** molecules in the COF-1 template, as shown in Figure S5. However, STM cannot unequivocally identify this architecture due to the relatively planar geometry of **CORA**, which makes it difficult to distinguish the pore-site **CORA**, in contrast to three-dimensional guests like fullerene.(43,44)

After the formation of a honeycomb-like trimer lattice, one more **CORA** can adsorb in the pore formed by **CORA**, as shown in Figure S6. We denote this adsorption site as raised-pore-site (RP-site). This architecture could be stabilized through two mechanisms: (i) if a **CORA** is adsorbed in the pore site, one more **CORA** can adsorb in the RP site through a **CORA–CORA** interaction;(52) (ii) with one or more solvent molecules in the COF-1 pore, which would prevent the formation of pore-site **CORA**, the RP-site can be stabilized through van der Waals interaction with the trapped solvent molecule(s) in the COF-1 pore.(53) When this adsorption occurs in a Phase I lattice (Figure 3a), the submolecular features of **CORA** in the RP-site are still distinguishable and suggest that the molecule has the same orientation as the rim-site **CORA**. This arrangement produces a parallel linear pattern(11) and gives a packing density of 2.12 molecules/nm^2. In contrast, the appearance of the RP-site **CORA** molecule in Phase II is brighter than the rim-site molecules. This is attributed to the Phase II pore having a different shape from Phase I, meaning that it cannot accommodate an in-plane **CORA** molecule. The **CORA** molecule may be trapped in a tilted geometry, or partially trapped with a different z-position from rim-site molecules, leading to a slight asymmetry in the appearance. Both of these periodic densely packed structures have been observed over a long-range (~50 nm, consistent with the domain size of COF-1),(41) as shown in Figure 3c,d. Although some defects can be observed in these long-range images, we attribute them to template defects, rather than to the inherent mismatch arising from five-fold symmetry.

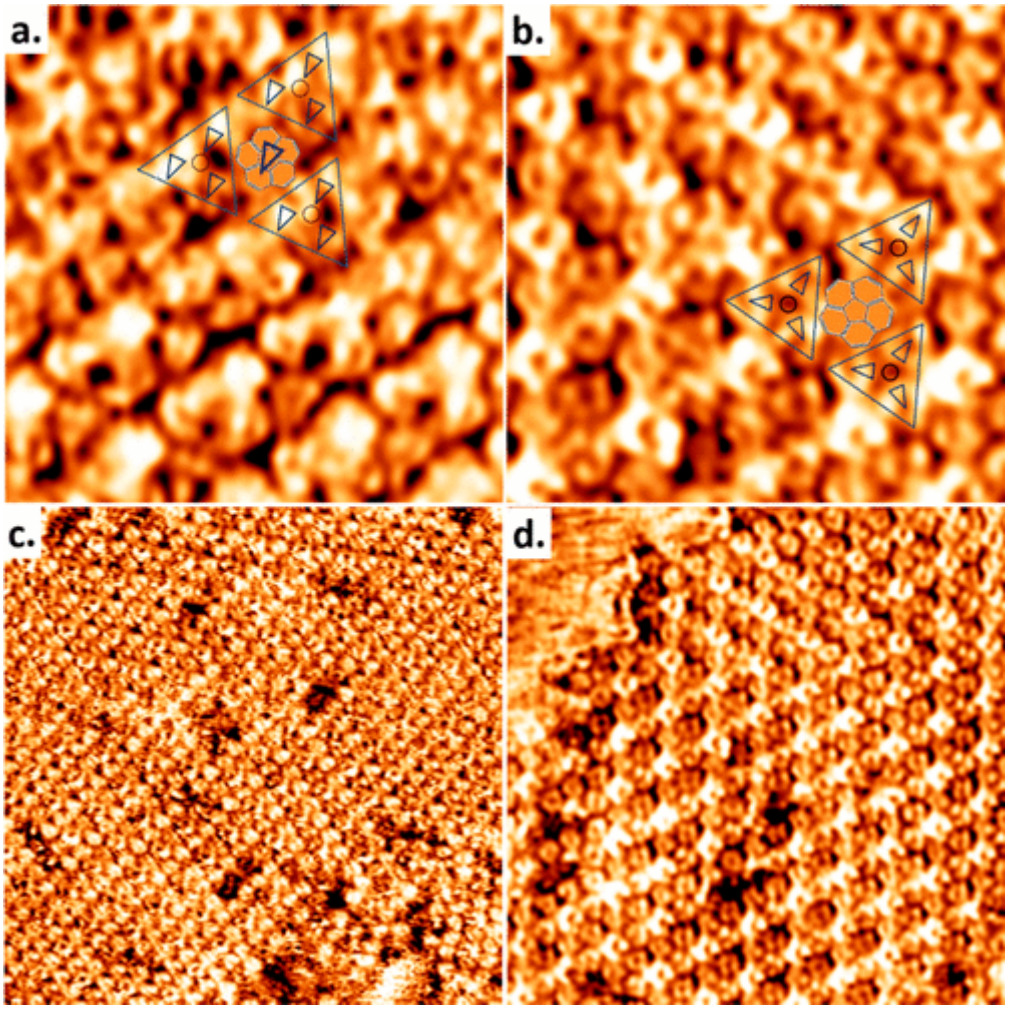

Figure 3. (a) STM image showing the adsorption of RP-site in a Phase I lattice. Image dimension: 5.9 × 5.9 nm^2. Tunneling conditions: V = −1800 mV, I = 50 pA. (b) STM image showing the adsorption of RP-site in a Phase II lattice. Image dimension: 6.0 × 6.0 nm^2. Tunneling conditions: V = −1800 mV, I = 50 pA. Sketches are superimposed on the STM images to show the positions and orientations of the **CORA** molecules. Large scale STM images showing Phase I (c) and phase II (d) periodic densely packing of **CORA** molecules. Image dimensions: 20.0 × 20.0 nm^2 (c) and 14.0 × 14.0 nm^2 (d). Tunneling conditions: (c) V = −1500 mV, I = 50 pA; (d) V = −1800 mV, I = 50 pA.

The COF-1 template imposes registry to well-defined positions on five-fold-symmetric adsorbate guest molecules, breaking through the limitations of the intrinsic lattice of preferred adsorption sites offered by a crystalline metal surface.(18,20) The defined corrugation of the template, compromising the interactions between dense contact five-fold molecules,(17) drives the formation of hierarchical assemblies with long-range periodic symmetry-reduced superstructures and a high packing density. The presence of solvent molecules in the COF-1 pore may prevent the formation of pore-site **CORA** and contribute to the stability of these high-density RP-site-containing **CORA** architectures.

Conclusions and Perspectives

We have shown that the COF-1 lattice presents two distinctive adsorption sites for the **CORA** guest molecules, pore-site, and rim-site. When coverage increases, the incompatibility of five-fold symmetry with the 2D plane is resolved in two distinct packing motifs and gives rise to unprecedented dense periodic structures. These results suggest that the template can act as external control to overcome the intrinsic symmetric mismatch between guest molecules and translational order. A range of novel potential dense supramolecular assemblies can be produced based on this method, where building blocks can own several different mismatch symmetries.

Experimental Section

Scanning tunneling microscopy (STM) was performed at room temperature at the solution/solid interface, using a Digital Instruments STM equipped with a Nanoscope IIIa controller. Tips were cut from a $Pt_{0.8}Ir_{0.2}$ wire (Nanoscience Instruments). Bias voltages are reported with respect to the STM tip. STM images were calibrated with the covalent organic framework (COF-1) lattice parameter (1.476 nm) using free WSxM software.(54) Model images were visualized by free Vesta software.(55)

Monolayer COF-1 on highly oriented pyrolytic graphite (HOPG) was formed using an established synthesis approach.(56) One milligram of 1,4-benzenediboronic acid (BDBA, Tokyo Chemical Industry Co. Ltd.) was added to 1.5 mL of heptanoic acid (99%, Sigma- Aldrich) and then sonicated for approximately 30 min. This produced a whitish suspension. Ten microliters of BDBA suspension was dropped onto freshly cleaved HOPG (Structure Probe International, grade SPI-1) and put into a reactor with a volume of ∼16 mL. One hundred thirty microliters of deionized water was added to the bottom of the reactor, and a valve to atmosphere was left slightly open to maintain an open system. The entire reactor was placed in an oven preheated to 125 °C and left for 60 min. After the thermal treatment, the reactor was taken out of oven and allowed to cool for at least 20 min before the samples were removed.

Afterward, 15 μL of corannulene (**CORA**. 97%, Tokyo Chemical Industry Co. Ltd.) in heptanoic acid was applied onto the substrate. Different concentrations had been used (8×10^{-6} M, 8×10^{-7} M, 8×10^{-8} M). All solution concentrations yield adsorption of **CORA.** We did not observe a strong concentration dependence in **CORA** density on COF-1 and anecdotally two different trimer motifs were observed in approximately equal proportion.

After introduction of a CORA solution with a concentration of 8×10^{-4} M onto clean HOPG, STM characterization did not show any molecular features or patterns, suggesting that CORA cannot self-assemble on HOPG alone.

Notes

The authors declare no competing financial interest.

Acknowledgments

Computations were performed on the tcs supercomputer at the SciNet HPC Consortium, funded by the Canada Foundation for Innovation under Compute Canada, the Government of Ontario, Ontario Research Fund – Research Excellence, and the University of Toronto. Computations were also made possible in part on the Cedar and Graham clusters of the shared Hierarchical Academic Research Computing Network (SHARCNET: www.sharcnet.ca) and Compute/Calcul Canada. J.M.M. acknowledges funding support from the Australian Research Council (DE170101170). F.R. is grateful to the Canada Research Chairs program for funding and partial salary support and also acknowledges NSERC for a Discovery Grant, Sichuan province for a 1000 talent short term award and the Government of China for a short term Chang Jiang scholar award.

References

1. Lörtscher, E. *Nat. Nanotechnol.* **2013**, *8* (6), 381, DOI: 10.1038/nnano.2013.105

2. Ratner, M. *Nat. Nanotechnol.* **2013**, *8* (6), 378, DOI: 10.1038/nnano.2013.110

3. Venkataraman, L.; Klare, J. E.; Nuckolls, C.; Hybertsen, M. S.; Steigerwald, M. L. *Nature* **2006**, *442* (7105), 904, DOI: 10.1038/nature05037

4. Guédon, C. M.; Valkenier, H.; Markussen, T.; Thygesen, K. S.; Hummelen, J. C.; Van Der Molen, S. J. *Nat. Nanotechnol.* **2012**, *7* (5), 305, DOI: 10.1038/nnano.2012.37

5. Xiang, D.; Wang, X.; Jia, C.; Lee, T.; Guo, X. *Chem. Rev.* **2016**, *116* (7), 4318– 4440, DOI: 10.1021/acs.chemrev.5b00680

6. Plass, K. E.; Grzesiak, A. L.; Matzger, A. J. *Acc. Chem. Res.* **2007**, *40* (4), 287– 293, DOI: 10.1021/ar0500158

7. Lück, R. *Mater. Sci. Eng., A* **2000**, *294-296*, 263– 267, DOI: 10.1016/S0921-5093(00)01302-2

8. Tomba, G.; Stengel, M.; Schneider, W.-D.; Baldereschi, A.; De Vita, A. *ACS Nano* **2010**, *4* (12), 7545– 7551, DOI: 10.1021/nn101884p

9. Jester, S.-S.; Sigmund, E.; Höger, S. *J. Am. Chem. Soc.* **2011**, *133* (29), 11062– 11065, DOI: 10.1021/ja203536t

10. Liu, J.; Lin, T.; Shi, Z.; Xia, F.; Dong, L.; Liu, P. N.; Lin, N. *J. Am. Chem. Soc.* **2011**, *133* (46), 18760– 18766, DOI: 10.1021/ja2056193

11. Tahara, K.; Balandina, T.; Furukawa, S.; De Feyter, S.; Tobe, Y. *CrystEngComm* **2011**, *13* (18), 5551– 5558, DOI: 10.1039/c1ce05336a

12. Ren, C.; Zhou, F.; Qin, B.; Ye, R.; Shen, S.; Su, H.; Zeng, H. *Angew. Chem., Int. Ed.* **2011**, *50* (45), 10612– 10615, DOI: 10.1002/anie.201101553

13. Taffs, J.; Royall, C. P. *Nat. Commun.* **2016**, *7*, 13225, DOI: 10.1038/ncomms13225

14. Wasio, N. A.; Quardokus, R. C.; Forrest, R. P.; Lent, C. S.; Corcelli, S. A.; Christie, J. A.; Henderson, K. W.; Kandel, S. A. *Nature* **2014**, *507* (7490), 86– 89, DOI: 10.1038/nature12993

15. Stöckl, Q.; Bandera, D.; Kaplan, C. S.; Ernst, K.-H.; Siegel, J. S. *J. Am. Chem. Soc.* **2014**, *136* (2), 606– 609, DOI: 10.1021/ja411279r

16. Zoppi, L.; Bauert, T.; Siegel, J. S.; Baldridge, K. K.; Ernst, K.-H. *Phys. Chem. Chem. Phys.* **2012**, *14* (38), 13365– 13369, DOI: 10.1039/c2cp41732d

17. Guillermet, O.; Niemi, E.; Nagarajan, S.; Bouju, X.; Martrou, D.; Gourdon, A.; Gauthier, S. *Angew. Chem., Int. Ed.* **2009**, *48* (11), 1970– 1973, DOI: 10.1002/anie.200805689

18. Bauert, T.; Merz, L.; Bandera, D.; Parschau, M.; Siegel, J. S.; Ernst, K.-H. *J. Am. Chem. Soc.* **2009**, *131* (10), 3460– 3461, DOI: 10.1021/ja8101083

19. Merz, L.; Parschau, M.; Siegel, J. S.; Ernst, K.-H. *Chimia* **2009**, *63* (4), 214– 216, DOI: 10.2533/chimia.2009.214

20. Parschau, M.; Fasel, R.; Ernst, K. H.; Gröning, O.; Brandenberger, L.; Schillinger, R.; Greber, T.; Seitsonen, A. P.; Wu, Y. T.; Siegel, J. S. *Angew. Chem., Int. Ed.* **2007**, *46* (43), 8258– 8261, DOI: 10.1002/anie.200700610

21. Theobald, J. A.; Oxtoby, N. S.; Phillips, M. A.; Champness, N. R.; Beton, P. H. *Nature* **2003**, *424* (6952), 1029– 1031, DOI: 10.1038/nature01915

22. Cicoira, F.; Santato, C.; Rosei, F. *Top. Curr. Chem.* **2008**, *285*, 203– 267, DOI: 10.1007/128_2008_2

23. Teyssandier, J.; De Feyter, S.; Mali, K. S. *Chem. Commun.* **2016**, *52* (77), 11465– 11487, DOI: 10.1039/C6CC05256H

24. den Boer, D.; Han, G. D.; Swager, T. M. *Langmuir* **2014**, *30* (3), 762– 767, DOI: 10.1021/la403807x

25. Griessl, S. J.; Lackinger, M.; Jamitzky, F.; Markert, T.; Hietschold, M.; Heckl, W. M. *J. Phys. Chem. B* **2004**, *108* (31), 11556– 11560, DOI: 10.1021/jp049521p

26. MacLeod, J. M.; Ivasenko, O.; Fu, C.; Taerum, T.; Rosei, F.; Perepichka, D. F. *J. Am. Chem. Soc.* **2009**, *131* (46), 16844– 16850, DOI: 10.1021/ja906206g

27. Stepanow, S.; Lingenfelder, M.; Dmitriev, A.; Spillmann, H.; Delvigne, E.; Lin, N.; Deng, X.; Cai, C.; Barth, J. V.; Kern, K. *Nat. Mater.* **2004**, *3* (4), 229– 233, DOI: 10.1038/nmat1088

28. Li, M.; Deng, K.; Lei, S. B.; Yang, Y. L.; Wang, T. S.; Shen, Y. T.; Wang, C. R.; Zeng, Q. D.; Wang, C. *Angew. Chem.* **2008**, *120* (35), 6819– 6823, DOI: 10.1002/ange.200802518

29. Rochford, L.; Jones, T.; Nielsen, C. *J. Phys. Chem. Lett.* **2016**, *7* (17), 3487– 3490, DOI: 10.1021/acs.jpclett.6b01656

30. Geng, Y.; Li, P.; Xue, J.; Luo, D.; Zhang, J.; Shu, L.; Deng, K.; Xie, J.; Zeng, Q. *Nano Res.* **2017**, *10* (3), 991– 1000, DOI: 10.1007/s12274-016-1358-5

31. MacLeod, J.; Ivasenko, O.; Perepichka, D.; Rosei, F. *Nanotechnology* **2007**, *18* (42), 424031, DOI: 10.1088/0957-4484/18/42/424031

32. Griessl, S. J.; Lackinger, M.; Jamitzky, F.; Markert, T.; Hietschold, M.; Heckl, W. M. *Langmuir* **2004**, *20* (21), 9403– 9407, DOI: 10.1021/la049441c

33. Ivasenko, O.; MacLeod, J. M.; Chernichenko, K. Y.; Balenkova, E. S.; Shpanchenko, R. V.; Nenajdenko, V. G.; Rosei, F.; Perepichka, D. F. *Chem. Commun.* **2009**, *10*, 1192– 1194, DOI: 10.1039/b819532c

34. Schull, G.; Douillard, L.; Fiorini-Debuisschert, C.; Charra, F.; Mathevet, F.; Kreher, D.; Attias, A.-J. *Nano Lett.* **2006**, *6* (7), 1360– 1363, DOI: 10.1021/nl060292n

35. Schull, G.; Douillard, L.; Fiorini-Debuisschert, C.; Charra, F.; Mathevet, F.; Kreher, D.; Attias, A. J. *Adv. Mater.* **2006**, *18* (22), 2954– 2957, DOI: 10.1002/adma.200600683

36. Lei, S.; Tahara, K.; Feng, X.; Furukawa, S.; De Schryver, F. C.; Müllen, K.; Tobe, Y.; De Feyter, S. *J. Am. Chem. Soc.* **2008**, *130* (22), 7119– 7129, DOI: 10.1021/ja800801e

37. Cui, D.; MacLeod, J.; Ebrahimi, M.; Perepichka, D.; Rosei, F. *Chem. Commun.* **2015**, *51* (92), 16510– 16513, DOI: 10.1039/C5CC07059G

38. Lei, S.; Surin, M.; Tahara, K.; Adisoejoso, J.; Lazzaroni, R.; Tobe, Y.; Feyter, S. D. *Nano Lett.* **2008**, *8* (8), 2541– 2546, DOI: 10.1021/nl8016626

39. Balandina, T.; Tahara, K.; Sändig, N.; Blunt, M. O.; Adisoejoso, J.; Lei, S.; Zerbetto, F.; Tobe, Y.; De Feyter, S. *ACS Nano* **2012**, *6* (9), 8381– 8389, DOI: 10.1021/nn303144r

40. Adisoejoso, J.; Tahara, K.; Okuhata, S.; Lei, S.; Tobe, Y.; De Feyter, S. *Angew. Chem.* **2009**, *121* (40), 7489– 7493, DOI: 10.1002/ange.200900436

41. Dienstmaier, J. r. F.; Gigler, A. M.; Goetz, A. J.; Knochel, P.; Bein, T.; Lyapin, A.; Reichlmaier, S.; Heckl, W. M.; Lackinger, M. *ACS Nano* **2011**, *5* (12), 9737– 9745, DOI: 10.1021/nn2032616

42. Diercks, C. S.; Yaghi, O. M. *Science* **2017**, *355* (6328), eaal1585, DOI: 10.1126/science.aal1585

43. Plas, J.; Ivasenko, O.; Martsinovich, N.; Lackinger, M.; De Feyter, S. *Chem. Commun.* **2016**, *52* (1), 68– 71, DOI: 10.1039/C5CC07557B

44. Cui, D.; Ebrahimi, M.; Rosei, F.; Macleod, J. M. *J. Am. Chem. Soc.* **2017**, *139* (46), 16732– 16740, DOI: 10.1021/jacs.7b08642

45. Cui, D.; MacLeod, J.; Ebrahimi, M.; Rosei, F. *CrystEngComm* **2017**, *19* (33), 4927– 4932, DOI: 10.1039/C7CE00263G

46. Stöckl, Q. S.; Hsieh, Y.-C.; Mairena, A.; Wu, Y.-T.; Ernst, K.-H. *J. Am. Chem. Soc.* **2016**, *138* (19), 6111– 6114, DOI: 10.1021/jacs.6b02412

47. Merz, L.; Parschau, M.; Zoppi, L.; Baldridge, K. K.; Siegel, J. S.; Ernst, K. H. *Angew. Chem., Int. Ed.* **2009**, *48* (11), 1966– 1969, DOI: 10.1002/anie.200804563

48. Scott, L. T.; Hashemi, M. M.; Bratcher, M. S. *J. Am. Chem. Soc.* **1992**, *114* (5), 1920– 1921, DOI: 10.1021/ja00031a079

49. Fujii, S.; Ziatdinov, M.; Higashibayashi, S.; Sakurai, H.; Kiguchi, M. *J. Am. Chem. Soc.* **2016**, *138* (37), 12142– 12149, DOI: 10.1021/jacs.6b04741

50. Gimzewski, J. K.; Joachim, C.; Schlittler, R. R.; Langlais, V.; Tang, H.; Johannsen, I. *Science* **1998**, *281* (5376), 531– 533, DOI: 10.1126/science.281.5376.531

51. Vidales, A. M.; Pugnaloni, L. A.; Ippolito, I. *Phys. Rev. E* **2008**, *77* (5), 051305, DOI: 10.1103/PhysRevE.77.051305

52. Bauert, T.; Baldridge, K. K.; Siegel, J. S.; Ernst, K.-H. *Chem. Commun.* **2011**, *47* (28), 7995– 7997, DOI: 10.1039/c1cc12540k

53. Lei, S.; Wang, C.; Wan, L.; Bai, C. *J. Phys. Chem. B* **2004**, *108* (4), 1173– 1175, DOI: 10.1021/jp037457q

54. Horcas, I.; Fernández, R.; Gomez-Rodriguez, J.; Colchero, J.; Gómez-Herrero, J.; Baro, A. *Rev. Sci. Instrum.* **2007**, *78* (1), 013705, DOI: 10.1063/1.2432410

55. Momma, K.; Izumi, F. J. *J. Appl. Crystallogr.* **2011**, *44* (6), 1272– 1276, DOI: 10.1107/S0021889811038970

56. Dienstmaier, J. r. F.; Medina, D. D.; Dogru, M.; Knochel, P.; Bein, T.; Heckl, W. M.; Lackinger, M. *ACS Nano* **2012**, *6* (8), 7234– 7242, DOI: 10.1021/nn302363d